BCSJ

Document type: Article

Article for Memorial Collection for CSJ/OUP Co-Operative Publication
Article for Controlled Chemical Construction (C3) for Advanced Functions

Carbon-Neutral Energy Cycle via Highly Selective Electrochemical Reactions Using Biomass Derivable Organic Liquid Energy Carriers

Takashi Fukushima,[1] Manabu Higashi,[2] and Miho Yamauchi*[2,3,4,5]

[1]Department of Applied Chemistry, Faculty of Engineering, Osaka Institute of Technology, 5-16-1 Ohmiya, Asahi-ku, Osaka 535-8585, Japan

[2]Institute for Materials Chemistry and Engineering (IMCE), 744 Motooka, Nishi-ku, Fukuoka 819-0395, Japan

[3]Advanced Institute for Materials Research (WPI-AIMR), Tohoku University, 2-1-1 Katahira, Aoba-ku, Sendai, Miyagi 980-8577, Japan

[4]Research Center for Negative Emissions Technologies (K-NETs), Kyushu University, 744 Motooka, Nishi-ku, Fukuoka 819-0395, Japan

[5]International Institute for Carbon-Neutral Energy Research (WPI-I2CNER), Kyushu University, 744 Motooka, Nishi-ku, Fukuoka 819-0395, Japan

E-mail: yamauchi@ms.ifoc.kyushu-u.ac.jp

Received: July 16, 2023; Accepted: September 10, 2023; Web Released: September 16, 2023

Takashi Fukushima
Takashi Fukushima received his Ph.D. degree under the guidance of Professor Koji Tanaka from Graduate University for Advanced Studies in 2008. Then, he worked at Institute for Molecular Science (IMS), Research Center for Materials Science (RCMS) Nagoya University, Institute for Integrated Cell-Material Sciences (iCeMS) Kyoto University, and Carbon-Neutral Energy Research (I^2CNER) Kyushu University. He is currently working at Osaka Institute of Technology as a lecturer. The current main subject of his research is development of catalysts for electrochemical synthesis of value-added organic compounds from sustainable feedstocks.

Miho Yamauchi
Miho Yamauchi received her Ph.D. under the guidance of Professor Ryuichi Ikeda from University of Tsukuba in 2001 and started research work as a technical staff there. She moved to Kyushu University as an assistant professor in 2003 and to Catalysis Research Center, Hokkaido University as an associate professor in 2008. In 2012, she joined International Institute for Carbon-Neutral Energy Research as a PI and moved to Institute for Materials Chemistry and Engineering, Kyushu University as a professor in 2022. Her research interests involve hydrogen related properties of metal nanoparticles, selective catalysis on structure controlled nanocatalysts and electrocatalysis for sustainable material production.

Abstract

Efficient storage and transport of electric energy is essential to promote the use of renewable energy based electricity. We demonstrate an energy cycle based on highly selective redox reactions between lactic acid (***Lac***) and pyruvic acid (***Pyr***), both of which are liquid under ambient conditions and can be obtained from biomass resources, thus realizing a completely low-emission system. As an energy storage device, an electrosynthesis cell (**LAEC**) for the production of ***Lac*** from ***Pyr*** was constructed using a membrane electrode assembly (MEA) consisting of a TiO_2 cathode catalyst for the electroreduction of ***Pyr*** and an IrO_x anode catalyst for water oxidation. Our **LAEC** achieved highly efficient ***Lac*** production from 10 M ***Pyr*** aqueous solution with Faradaic efficiency (FE) of approximately 100% in the applied voltage range of 1.4–2.4 V, resulting in an energy conversion efficiency of 50% and a current density of $-0.4\ A\ cm^{-2}$ at 2.0 V. Direct ***Lac*** fuel cell (**DLAFC**) was also constructed and its FE values for the ***Pyr*** production reached approximately 100%, enabling direct electronic energy storage in bio-derivative liquid carriers and efficient energy circulation with minimal CO_2 emissions.

Keywords: Carbon-neutral energy circle | Organic liquid carriers | Redox reactions

1. Introduction

The use of renewable energy sources, such as solar, wind, wave, etc., is obviously important to overcome the dependence on fossil resources and the problem of global warming; however, the intermittent nature and uneven distribution of renewable energy sources hinders their practical and effective use. Therefore, effective energy storage and transport by converting electricity made from renewable energy sources into energy-storable chemicals, i.e. energy carriers, is expected to play an essential role in the use of renewable energy sources.[1–14]

Hydrogen is the cleanest and a sustainable energy carrier, and industrial technologies for both electrochemical hydrogen production and electricity generation from hydrogen have reached maturity.[1–4] For instance, the high energy conversion efficiency (η_H) of 67–82%[15,16] for electrochemical hydrogen production has already been realized by commercial water electrolyzers, and fuel cell vehicles employing hydrogen as a fuel are provided by several global manufacturers. However, hydrogen has some potential disadvantages, such as a quite low energy density of 12.8 MJ m^{-3} at standard ambient temperature and pressure (SATP) and a highly explosive nature, and therefore the additional energy consuming processes, such as compression, liquefaction, and chemical conversion into hydrogen-containing compounds,[17–24] are required for storing and transporting hydrogen.

Alcohols are generally chemically stable liquid or solid at SATP, and therefore have several advantages as an energy carrier, including ease of storage, transport and handling, as well as higher volumetric energy density. Recently, we have successfully constructed a carbon neutral energy cycling system using a redox couple of alcohol/carboxylic acid or alcohol/ketone, where electric power is stored via electroreduction of acids or ketones, and generated via electrooxidation of an alcohol.[25–28] Thus, electric power circulation is achievable without CO_2 emission.[29] In principle, carboxylic acids are chemically stable and difficult to electrochemically reduce to form alcoholic compounds.[30] Meanwhile, we have found that oxalic acid (HOOC–COOH), a divalent carboxylic acid, can be highly selectively reduced to its alcoholic compound, namely, glycolic acid (HOOC–CH_2OH), via 4-electron reduction on anatase TiO_2, even in aqueous solution, which is the first report of electrochemical alcohol production from an acid.[31] Furthermore, the stored electricity can be extracted via Pt-catalyzed "CO_2-free" electrooxidation of glycolic acid to form oxalic acid,[29] demonstrating a carbon neutral energy circle based on the redox reaction between an alcohol and an acid.[31] In addition, we have newly fabricated a flow-type polymer electrolyzer with a TiO_2 cathode catalyst, called a polymer electrolyte alcohol electrosynthesis cell (PEAEC), and demonstrated the continuous electrochemical reduction of 3 M oxalic acid to form glycolic acid using the PEAEC without the addition of electrolyte to the reaction solution.[32,33] The common state of oxalic acid is solid, and its electrochemical conversion processes takes place in aqueous solution, which limits availability as an energy carrier; the operation temperature should be high enough, 50–80 °C, to avoid precipitation and enhance the reaction rate. The use of a liquid redox couple under ambient conditions is therefore highly desired. We then surveyed redox couples that are reactive on TiO_2 and found that a 2-electron reduction of keto group on some α-keto acids proceeds preferentially on anatase TiO_2.[34–36] Interestingly the reactivity of α-keto acids depends on the relative position between the lowest unoccupied states of TiO_2 and that of α-keto acid and the adsorption states of the carboxy group on TiO_2.[34,35,37,38] These findings have initiated other application such as light assisted alcohol production,[39] electrochemical amino acid production from organic acids and nitrogen sources[40–43] and thermoelectric conversion using biocompatible organic acids at ambient temperatures.[44] Among the reactive redox couples, lactic acid ($CH_3CH(OH)COOH$, ***Lac***) and pyruvic acid ($CH_3C(=O)$-COOH, ***Pyr***) appear to be a favorable combination due to their liquid nature under ambient conditions.

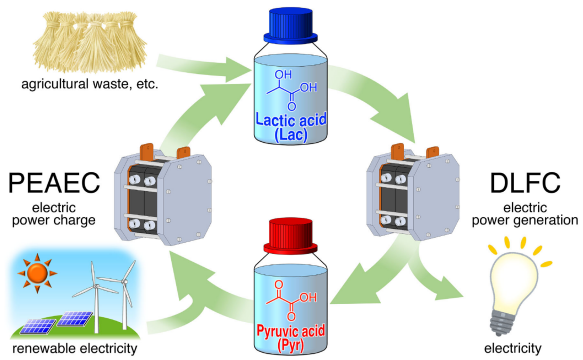

Figure 1. Scheme of a carbon-neutral electric energy cycle using lactic acid and pyruvic acid as bio-derivable liquid carriers.

Lac and ***Pyr*** are compounds that play a vital role in biological metabolism, forming an alcohol/ketone redox couple. Both of them are liquid at SATP and fully miscible with water, meeting energy carrier requirements. In addition to these preferable properties, they also have the advantage of being produced from non-petroleum sources. Currently, most ***Lac*** is produced by microbial fermentation of sugars and starches,[45,46] and furthermore, recent advances in the fermentation technology make it possible to use non-food-competing biomass, such as agricultural waste, as a feedstock for ***Lac*** production.[47–50] In addition, we have recently found that a Ti mesh and felt covered with anatase TiO_2 nanocrystals (TiO_2/Ti_{mesh} and TiO_2/Ti_{felt}) exhibit excellent catalytic ability to reduce oxalic acid to glycolic acid,[33] which led us to construct a new liquid carrier-mediated energy circulation system utilizing the ***Lac***/***Pyr*** redox couple (Figure 1). In this work, we demonstrate highly selective ***Lac*** production from 10 M ***Pyr*** with nearly FE = 100% on a newly constructed electrochemical synthesis cell (**LAEC**), where the hydrogen evolution reaction (HER) is completely suppressed even in highly acidic aqueous solution. We then achieved a remarkably high reduction rate (or current density, j) of 490 mA cm^{-2} at 2.0 V. A direct ***Lac*** fuel cell (**DLAFC**) was also constructed to generate electricity using ***Lac*** as a fuel. **DLAFC** using 1 M ***Lac*** was found to exhibit selective oxidation of ***Lac*** to ***Pyr***. The combination of such highly selective electrochemical reactions in **LAEC** and **DLAFC** potentially completes a

carbon-neutral energy cycle in which electrical energy is directly stored in and generated from bio-derivable liquid carriers.

2. Result and Discussion

2.1 Optimization of Electrode Structures in LAEC. We first assembled **LAEC** with TiO_2/Ti_{mesh} and two TiO_2/Ti_{felt} as a cathode (Figure 2a) and lab-made IrO_2 nanoparticles as an anode catalyst (3 mg cm^{-2}). 1 M ***Pyr*** aqueous solution and pure water were passed through the cathode and the anode sides, respectively, at 0.5 mL min^{-1}. The cathode outlet solution from **LAEC** was analyzed at every applied potential by HPLC and ^{1}H NMR to determine products and estimate Faradaic efficiencies (FEs) for each product formation (see SI). Although we could not observe efficient reduction of oxalic acid on TiO_2 below 50 °C, ***Lac*** was produced from ***Pyr*** even at 25 °C (Figure S1). This is because the kinetics of 2-electron reduction for the ***Lac*** formation is faster than that of two-step 2-electron reduction of oxalic acid.[29] In addition, a relatively stable current flow was observed during the **LAEC** operation, implying high robustness of the catalyst and electrode. Considering that energy density of 1 M ***Lac*** is 204 MJ m^{-3} in the case of the selective oxidation of ***Lac*** to ***Pyr***, which is much smaller than 1,892 MJ m^{-3} of 3 M oxalic acid, we then tried to increase concentration of the ***Pyr*** solution for **LAEC** application. Figure S2 shows j and FE values in electrochemical reduction of 1, 3 and 6 M ***Pyr*** at 25 °C. In all experiments, j values were approximately 150 mA cm^{-2} at 2.8 V, whereas FE was increased especially in the flow of higher-concentration ***Pyr*** at lower voltages,

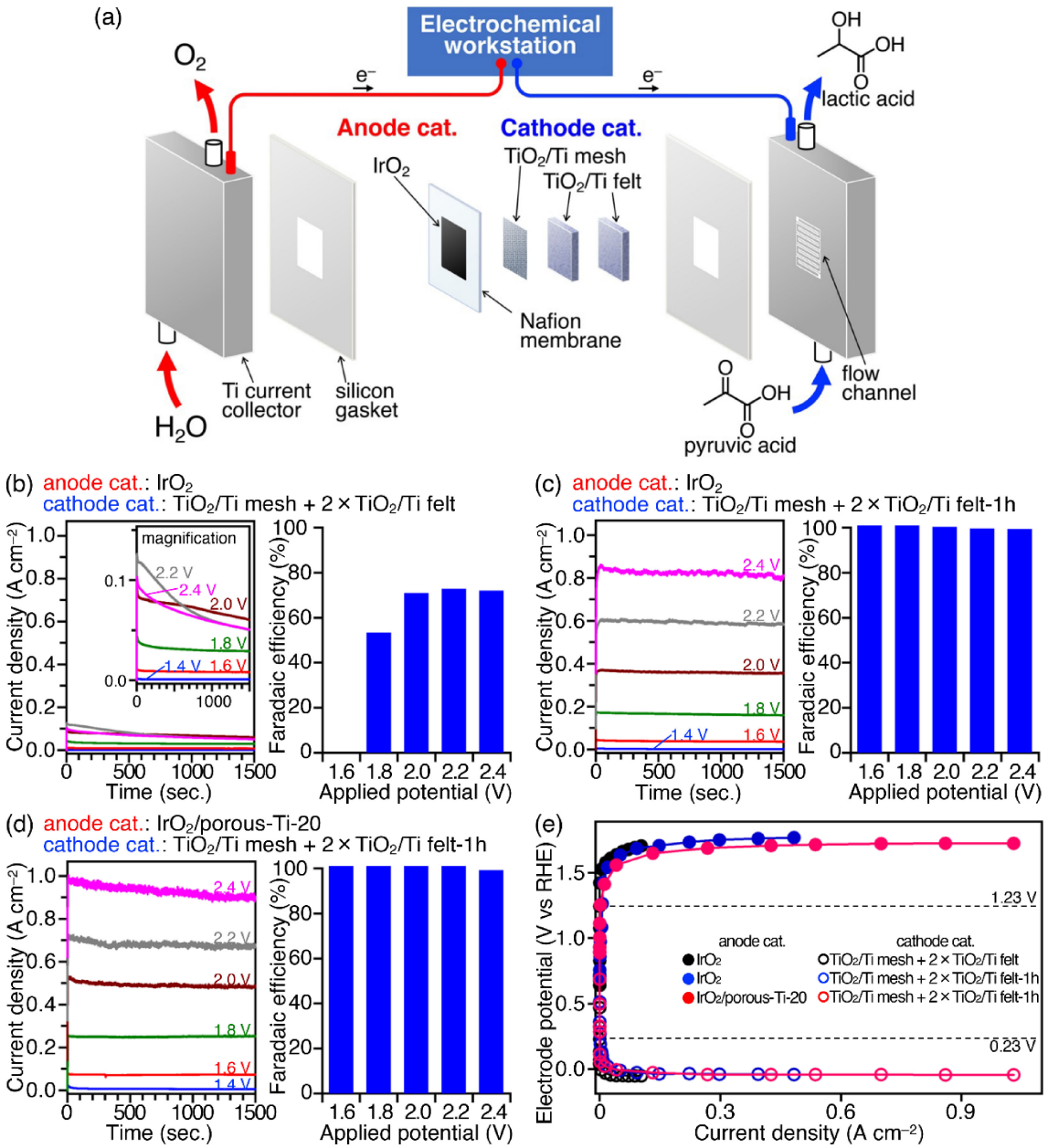

Figure 2. (a) Structure of **LAEC**. (b)–(d) Current density (left) and Faradaic efficiency (right) for ***Lac*** production by feeding 10 M ***Pyr*** and 0.5 M H_2SO_4 into **LEAC** equipped with various cathode and anode catalysts at 50 °C. Cathode and anode catalysts used are shown above the graph. (e) Cathodic (empty circle) and anodic (filled circle) polarization curves of **LEAC**.

suggesting that the reaction rate is limited by the number of catalytic sites at 25 °C and the selectivity depends on the contact probability of substrates. To increase the reaction rate, we designed a new cathode structure by stacking a TiO_2/Ti_{mesh} and two TiO_2/Ti_{felt} electrodes on a membrane by considering transport of electrolyte solution (Figure 2a). We also increased ***Pyr*** concentration to 10 M, equivalent to 2,040 MJ m^{-3}, raised reaction temperature to 50 °C and operated **LAEC** at different applied voltages in the range 1.4 to 2.4 V, with 10 M ***Pyr*** and water fed to the cathode and anode at 0.5 mL min^{-1}. Figure 2b shows a relatively stable current flow during the operation, illustrating the high robustness of the catalysts. In addition, reasonably high FEs of 53–73% were obtained for ***Lac*** production at 1.8–2.4 V. The observed j values such as 72 mA cm^{-1} at 2.0 V were higher than those obtained in recent work using a PEAEC operated with 1 M oxalic acid and similar setup; j = 44 mA cm^{-1} at 2.0 V. Nevertheless, **LAEC** operated with 10 M ***Pyr*** showed cell resistance of 2.8 Ω, considerably larger than 0.40 Ω with 1 M oxalic acid. We thought this might be due to small water content of 10 M ***Pyr*** solution and smaller ionization degree of ***Pyr*** than that of oxalic acid (*cf.* pK_a of ***Pyr*** and oxalic acid are 2.5[51] and 1.2,[52] respectively). We thus added H_2SO_4 to the cathode solution and use of TiO_2/Ti felts with a thinner TiO_2 layer to decrease the cell resistance, resulting in a smaller cell resistance of 1.6 Ω and then higher j of 120 mA cm^{-1} at 2.0 V (Figure S3a). Furthermore, FEs for ***Lac*** production became almost 100% at 1.6–2.4 V, indicating that the highly acidic environment brought by the H_2SO_4 addition in the cathode solution prevents ionization of ***Pyr*** and this facilitates adsorption of ***Pyr*** on TiO_2 surface by weakening electrostatic repulsion of the anion form. We further optimized the preparation conditions of the cathode. To reduce the cell resistance, we prepared TiO_2/Ti_{felt} with a thin TiO_2 layer by controlling the reaction time in the first hydrothermal treatment to be 1 and 3 h (TiO_2/Ti_{felt}-1h and TiO_2/Ti_{felt}-3h). The use of the newly prepared cathodes effectively decreased the cell resistance and increased j values of **LAEC**; 0.71 Ω and j = 360 mA cm^{-1} on TiO_2/Ti_{felt}-1h, and 1.0 Ω and 290 mA cm^{-1} on TiO_2/Ti felts-3h at 2.0 V (Figures 2c and S3b). We also tested **LAEC**s in which TiO_2/Ti_{mesh} and TiO_2/Ti_{felt} were replaced by staring Ti mesh and Ti felt, respectively (Figure S3c). It should be noted that **LAEC** with the Ti mesh showed lower resistance of 0.36 Ω, but exhibited lower j and lower selectivity than those observed on TiO_2/Ti_{mesh} and two TiO_2/Ti_{felt}-1h; 220 mA cm^{-2} at 2.0 V and FE = 40–95% for ***Lac*** production at 1.6–2.4 V (Figure S3c), indicating enhancement of HER on the metallic Ti electrode. Consequently, TiO_2/Ti_{mesh} with two TiO_2/Ti_{felt}-1h is the best the cathode composition in this work. We have also improved anode catalysts. We originally prepared the anode of **LAEC** by spraying an IrO_2 ink containing lab-made IrO_2 nanoparticles (see SI), Nafion solution, 2-propanol and water onto a Nafion membrane and then hot-pressing the IrO_2-loaded Nafion membrane with TiO_2 cathodes (see SI). However, this method limits loading amount of IrO_2 catalyst per reaction area and a thick IrO_2 layer behaves as a resistance for water diffusion. To increase the IrO_2 loading amount while maintaining sufficient water diffusivity, we designed a new anode consisting of IrO_2 particles deposited on a thick porous Ti plate (porous-Ti, 0.5 mm thickness), which has large surface area for catalyst loading and high water permeability as well as high electrical conductivity and corrosion resistance. The amount of IrO_2 loading was increased by repeating the dipping process, and finally, 10, 20, and 40 mg cm^{-2} of IrO_2 loading were achieved (IrO_2/porous-Ti-10, 20, and 40, respectively). SEM images of the surface of the porous-Ti and the IrO_2/porous-Ti anodes indicated that the pores of IrO_2/porous-Ti-10, 20, and 40 are occupied by the agglomerates of IrO_2 particles, and the porosity decreased with the increase of the IrO_2 loading amount (Figures 3b–d). TEM observations represented that IrO_2 particles on the IrO_2/porous-Ti anodes have extremely small sizes around 1–2 nm regardless of loading amounts of IrO_2 on porous-Ti materials (Figures 3e–g). We then applied IrO_2/porous-Ti anodes to **LAEC**s equipped with the cathode consisting of one TiO_2/Ti_{mesh} and two TiO_2/Ti_{felt}-1h and evaluated their performance (Figure S4a for IrO_2/porous-Ti-10, Figure 2d for

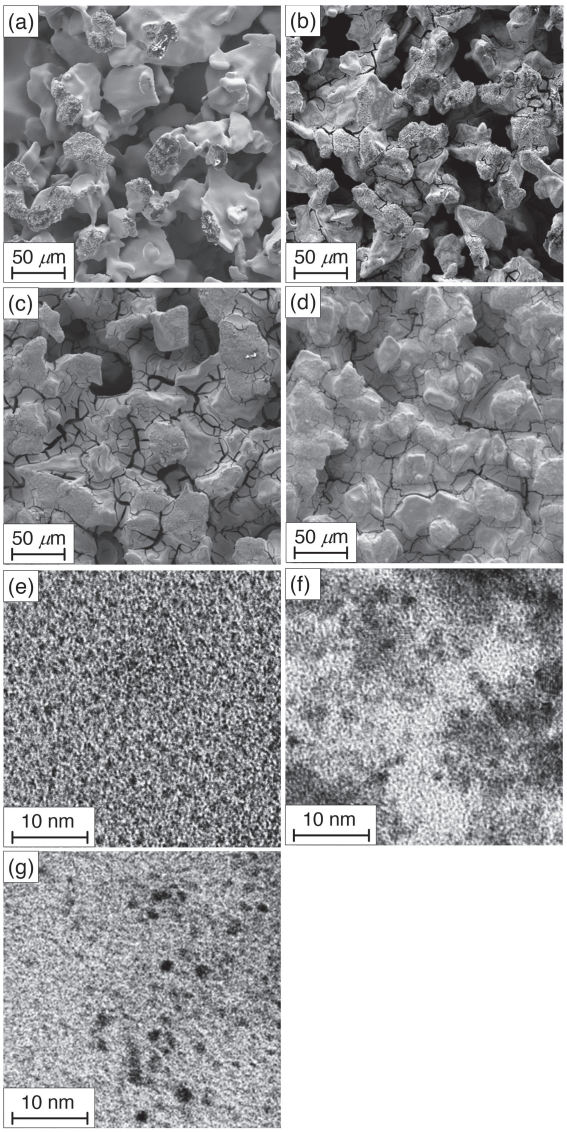

Figure 3. SEM images of the surface of (a) porous-Ti, (b) IrO_2/porous-Ti-10, (c) IrO_2/porous-Ti-20 and (d) IrO_2/porous-Ti-40, and TEM images of powder samples collected from (e) IrO_2/porous-Ti-10, (f) IrO_2/porous-Ti-20 and (g) IrO_2/porous-Ti-40.

IrO_2/porous-Ti-20 and Figure S4b for IrO_2/porous-Ti-40). **LAEC**s with IrO_2/porous-Ti-10 and 20 showed an increase in j values; 410 and 490 mA cm^{-1} at 2.0 V, respectively, depending on the IrO_2 loading amount. Meanwhile, the performance on IrO_2/porous-Ti-40 was no better than that of the former; 410 mA cm^{-1} at 2.0 V, which is probably ascribed to the reduced permeability of water into the anode resulting from the blocking of pores of Ti by IrO_2 particles. Accordingly, IrO_2/porous-Ti-20 exhibited the highest performance.

To evaluate the overpotentials for the cathode and anode reactions, we measured the electrode potentials during operation using a cell with a reference electrode. Figure 2e represents polarization curves of **LAEC** composed of three different electrode combinations to compare their performance; IrO_2 nanoparticles for an anode and (i) one TiO_2/Ti_{mesh} and two TiO_2/Ti_{felt} (black), or (ii) one TiO_2/Ti_{mesh} and two TiO_2/Ti felts-1h (blue) for a cathode, and (iii) IrO_2/porous-Ti-20 for an anode and one TiO_2/Ti_{mesh} and two TiO_2/Ti felts (red). The overpotential was calculated from the difference between a thermodynamically determined equilibrium potential; 0.23 V for the cathode reaction and 1.23 V for the anode reaction, and an experimentally observed electrode potential. The anode and cathode overpotentials were compared at $j = 100$ mA cm^{-1}. We then found that application of TiO_2/Ti_{felt}-1h for TiO_2/Ti_{felt} (ii) does not change over anodic potential so much; 0.28 V (Figure 2e, black, i) to 0.26 V (Figure 2e, blue, ii), whereas the use of the IrO_2/porous-Ti-20 anode (iii) greatly reduces the anodic overpotential from 0.46 V (Figure 2e, blue, ii) to 0.39 V (Figure 2e, red, iii). The energy conversion efficiency of **LAEC** (η_{LAEC}), which indicates the ratio between electrical energy input and chemical energy stored in ***Lac***, can be calculated using following equation:

$$\eta_{LAEC} = \frac{E_{LAEC} \times FE_{Lac}}{E_{appl}},$$

where E_{appl} is the applied voltage, FE_{Lac} is the FE for ***Lac*** production and E_{LAEC} is the theoretical electrolysis voltage for **LAEC** operation (1.0 V) calculated from the standard redox potentials of ***Lac*** production from ***Pyr*** (0.23 V) and water oxidation (1.23 V). According to this equation, η_{LAEC} on the **LAEC** showing the highest performance (Figure 2d) was calculated to be $\eta_{LAEC} = 50\%$ at 2.0 V. These values are nearly comparable to those for recent commercial polymer electrolyte membrane (PEM) water electrolyzers (current density: 0.6–2.0 A cm^{-2}, efficiency: 67–82%),[15,16] demonstrating the potential of **LAEC** for practical use as an electronic energy storage device.

2.2 Construction of DLAFC. **DLAFC** was fabricated using commercial Pt/C and Pt-Ru/C catalysts as the cathode and anode catalysts, respectively. The catalysts were loaded on porous carbon papers by brushing a catalyst ink prepared using above mentioned catalysts, Nafion solution and water. The catalyst loaded carbon papers (Pt/C/C paper and Pt-Ru/C/C paper, SI) were placed on each side of a Nafion membrane and hot-pressed to make an MEA (Figure 4a, SI). The prepared MEA was sandwiched between two Ti current collectors having flow channels to form **DLAFC**. We first tested the performance of **DLAFC** using Pt/C as a cathode catalyst (10 mg cm^{-2} Pt, 1 cm^2), and Pt-Ru/C as an anode (10 mg cm^{-2} Pt-Ru, 1 cm^2) at 80 °C by flowing wet oxygen gas (relative humidity 80%,

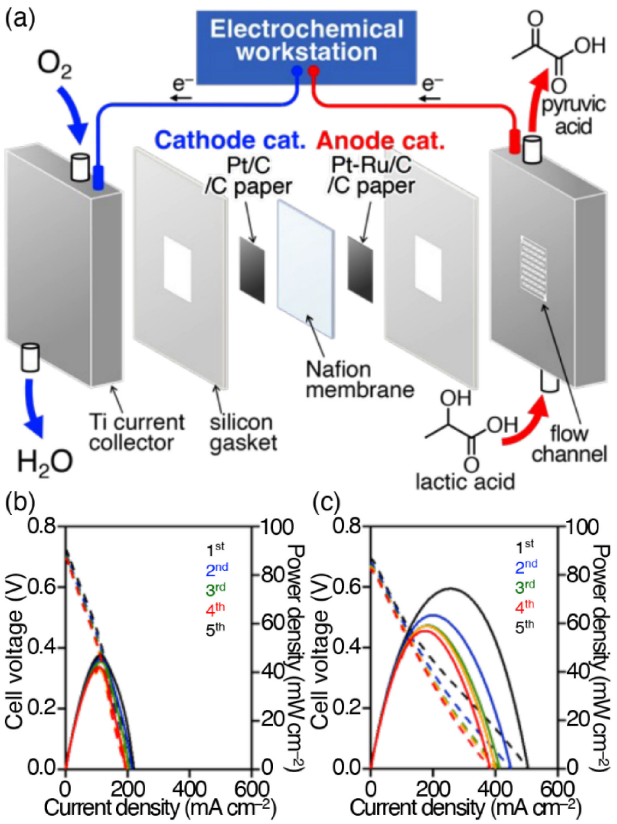

Figure 4. (a) A schematic diagram of **DLAFC**. Polarization curves (broken) and power density curves (solid) for **DLAFC** using 1 M ***Lac*** at 80 °C. Total metal loading on an anode and a cathode was (b) 20 and (c) 80 mg cm^{-2}.

90 sccm) and 1 M ***Lac*** aqueous solution (0.5 mL min^{-1}) into the cathode and the anode, respectively. Figure 4b represents polarization curves and power density curves for **DLAFC**. The measurements were repeated five times, and each of the measurements gave similar polarization curves, indicating the good stability of the catalysts. The open circuit voltage of 0.72 V was smaller than the theoretical value of 1.00 V by 0.28 V (28%), which is similar to that for the typical H_2/O_2 proton-exchange membrane fuel cell,[53] indicating that use of an acidic membrane may prevent a rapid ***Lac*** crossover. The power density curves indicate that **DLAFC** can generate electric power with 45 mW cm^{-2} of power density at the maximum. We then subsequently operated the **DLAFC** at a constant voltage of 0.4 V. The time course of the current density (Figure S5a) elucidates that **DLAFC** has sufficient ability to steadily give current flow with density of approximately 20 mA cm^{-2} during 25 min operation. The HPLC analysis of the anode outlet solution revealed that ***Lac*** was selectively oxidized to form ***Pyr*** with 99% (almost 100%) FE. Thus, carbon neutral energy circulation using a combination of **LAEC** and **DLAFC** is achievable by using 1 M ***Lac*** and ***Pyr*** solutions. We then aimed at enhancement of **DLAFC** performance by increasing amounts of the cathode and anode catalysts. The double-layered structure was employed for increasing catalyst loading on the MEA. The catalyst ink containing Pt-Ru/C catalyst was sprayed on Teflon film to form Pt-Ru/C/Teflon film. Then, two pieces of Pt-Ru/C/Teflon film were placed on each side of Nafion membrane

and hot-pressed. The resulting Pt-Ru/C loaded Nafion membrane was sandwiched with above-mentioned Pt/C/C paper and Pt-Ru/C/C paper and hot-pressed to yield a MEA. We evaluated the performance of **DLAFC** equipped with the new MEA (1 cm^2) consisting of Pt/C/C paper (20 mg cm^{-2} Pt) and Pt-Ru/C (20 mg cm^{-2} Pt-Ru) at the cathode, and Pt-Ru/C/C paper (20 mg cm^{-2} Pt-Ru) and Pt-Ru/C (20 mg cm^{-2} Pt-Ru) at the anode. Note that the total of metal loading at the cathode and the anode was increased to 80 mg cm^{-2} from 20 mg cm^{-2} by using the new MEA. The open circuit voltage of 0.70 mV on the **DLAFC** with the new MEA (Figure 4c) was comparable to that on the **DLAFC** with the previous MEA (Figure 4b), whereas the maximum power density of the **DLAFC** was increased to 74 mW cm^{-2} by increasing amounts of the catalysts. This value is comparable to those reported for direct liquid fuel cells, such as direct methanol fuel cell (DMFC, 50–200 mW cm^{-2} at 70–90 °C).[53] Unfortunately, the power density decreased with each measurement, and finally the maximum power density was decreased to 57 mW cm^{-2}, which is probably ascribed to corrosion of the Pt-Ru/C catalyst on the anode caused by the acidic anode solution. A constant potential operation of the **DLAFC** at 0.4 V gave stable current density of approximately 60 mA cm^{-2} during 25 min operation (Figure S5b) and resulted in the formation of ***Pyr*** with FE of 84%. As a by-product, acetic acid which would be formed by electrochemical 4-electron oxidation of ***Lac*** (Figure S6a) was detected with FE of 5.9%. We could not find any other products in the solution phase although the sum of FE values for the two products is 89.9%. This indicates that acetic acid undergoes further redox conversions to form gaseous products. One possible candidate for such gas evolution reactions is Kolbe electrolysis which can convert acetic acid into ethane and CO_2 (Figure S6b). Thus, further improvement of the anode will enhance the availability of **DLAFC**.

10 M ***Lac*** with its high energy density of 2,036 MJ m^{-3} has a great advantage when selectively oxidized to ***Pyr***. We then performed **DLAFC** with 10 M ***Lac*** (Figure S7a). In this experiment, the open circuit potential was approximately 0.77 V and the maximum power density was 19 mW cm^{-2}, which decreased significantly with repetition. We performed chronoamperometry using the same **DLAFC** setup at 0.4 V and obtained a stable current flow of 20 mA cm^{-2} for 1500 s and determined approximately 100% of FE for ***Pry*** production (Figure S7b). Although much improvement is needed, a 10 M ***Lac***/***Pyr*** system will be achievable.

3. Conclusion

In the present work, we demonstrated for the first time the electric energy circulation system using a ***Lac***/***Pyr*** redox couple as a liquid energy carrier. The electric energy storage via electrochemical reduction of ***Pyr*** to ***Lac*** was performed using the **LAEC** equipped with our specially-developed TiO_2/Ti mesh, felt and IrO_2/porous-Ti catalysts on the cathode and anode, respectively. We achieved high efficiency for ***Lac*** production from 10 M ***Pyr*** using **LAEC**.

For electric power generation via electrooxidation of ***Lac*** to ***Pyr***, we fabricated **DLAFC** using Pt(-Ru)/C electrocatalyst and showed that **DLAFC** is capable of power generation from 1 M ***Lac*** with 45 mW cm^{-2} of the maximum power density and FE = 100% for the production of ***Pyr***. It should be noted that electrooxidation of ***Lac*** with FE = 100% towards ***Pyr*** means that carbon-neutral power generation and thus carbon-neutral energy cycling with **LAEC**/**DLAFC** are achievable. The **LAEC**/**DLAFC** system has the advantage that it does not involve high temperature conversions above 100 °C and the processing of gaseous carriers, thus realizing a compact system with low energy consumption. We hope that our findings will contribute to the effective use of renewable electricity and to the creation of a sustainable society in the future.

We acknowledge funding from JST-CREST (15656567) and JSPS KAKENHI (JP18H05517, 22K19088, JP19H05062, JP22H01758, 23H00313). The authors thank Prof. Ryu Abe, Kyoto University and Prof. Tatsuya Takeguchi, Iwate University for their kind guidance.

Supporting Information

Experimental details and additional figures are shown in the Supporting Information. This material is available on https://doi.org/10.1246/bcsj.20230172.

References

1 K. T. Moller, T. R. Jensen, E. Akiba, H. W. Li, *Prog. Nat. Sci.* **2017**, *27*, 34.
2 S. E. Hosseini, M. A. Wahid, *Renewable Sustainable Energy Rev.* **2016**, *57*, 850.
3 K. Mazloomi, C. Gomes, *Renewable Sustainable Energy Rev.* **2012**, *16*, 3024.
4 A. Zuttel, A. Remhof, A. Borgschulte, O. Friedrichs, *Philos. Trans. R. Soc., A* **2010**, *368*, 3329.
5 B. H. R. Suryanto, H. L. Du, D. B. Wang, J. Chen, A. N. Simonov, D. R. MacFarlane, *Nat. Catal.* **2019**, *2*, 290.
6 C. X. Guo, J. R. Ran, A. Vasileff, S. Z. Qiao, *Energy Environ. Sci.* **2018**, *11*, 45.
7 M. H. Hasan, T. M. I. Mahlia, M. Mofijur, I. M. R. Fattah, F. Handayani, H. C. Ong, A. S. Silitonga, *Energies* **2021**, *14*, 3732.
8 M. Bevilacqua, J. Filippi, H. A. Miller, F. Vizza, *Energy Technol.* **2015**, *3*, 197.
9 B. Kumar, V. Atla, J. P. Brian, S. Kumari, T. Q. Nguyen, M. Sunkara, J. M. Spurgeon, *Angew. Chem., Int. Ed.* **2017**, *56*, 3645.
10 R. Kortlever, I. Peters, S. Koper, M. T. M. Koper, *ACS Catal.* **2015**, *5*, 3916.
11 K. Matsuoka, K. Miyoshi, Y. Sato, *J. Power Sources* **2017**, *343*, 156.
12 S. Mitsushima, Y. Takakuwa, K. Nagasawa, Y. Sawaguchi, Y. Kohno, K. Matsuzawa, Z. Awaludin, A. Kato, Y. Nishiki, *Electrocatalysis* **2016**, *7*, 127.
13 Y. Inami, S. Iguchi, S. Nagamatsu, K. Asakura, I. Yamanaka, *ACS Omega* **2020**, *5*, 1221.
14 M. Yamauchi, R. Watanabe, S. Hata, S. Kitano, M. Sadakiyo, T. Takeguchi, *Electrosynth. Fuels* **2017**, *4*, 17.
15 I. Dincer, C. Acar, *Int. J. Hydrogen Energy* **2015**, *40*, 11094.
16 M. David, C. Ocampo-Martinez, R. Sanchez-Pena, *J. Energy Storage* **2019**, *23*, 392.
17 T. He, P. Pachfule, H. Wu, Q. Xu, P. Chen, *Nat. Rev. Mater.* **2016**, *1*, 16059.
18 Y. Kojima, *Int. J. Hydrogen Energy* **2019**, *44*, 18179.
19 M. Yadav, Q. Xu, *Energy Environ. Sci.* **2012**, *5*, 9698.

20 P. Preuster, C. Papp, P. Wasserscheid, *Acc. Chem. Res.* **2017**, *50*, 74.
21 K. Muller, K. Stark, B. Muller, W. Arlt, *Energy Fuels* **2012**, *26*, 3691.
22 Y. Wu, Y. Qi, J. Chen, H. Fu, J. Zheng, X. G. Li, *RSC Adv.* **2016**, *6*, 103299.
23 W. T. Wang, J. M. Herreros, A. Tsolakis, A. P. E. York, *Int. J. Hydrogen Energy* **2013**, *38*, 9907.
24 A. K. Figen, M. B. Piskin, B. Coskuner, V. Imamoglu, *Int. J. Hydrogen Energy* **2013**, *38*, 16215.
25 T. Matsumoto, M. Sadakiyo, M. L. Ooi, S. Kitano, T. Yamamoto, S. Matsumura, K. Kato, T. Takeguchi, M. Yamauchi, *Sci. Rep.* **2014**, *4*, 1.
26 T. Matsumoto, M. Sadakiyo, M. L. Ooi, T. Yamamoto, S. Matsumura, K. Kato, T. Takeguchi, N. Ozawa, M. Kubo, M. Yamauchi, *Phys. Chem. Chem. Phys.* **2015**, *17*, 11359.
27 M. Yamauchi, N. Ozawa, M. Kubo, *Chem. Rec.* **2016**, *16*, 2249.
28 N. Ozawa, S. Chieda, Y. Higuchi, T. Takeguchi, M. Yamauchi, M. Kubo, *J. Catal.* **2018**, *361*, 361.
29 T. Fukushima, S. Kitano, S. Hata, M. Yamauchi, *Sci. Technol. Adv. Mater.* **2018**, *19*, 142.
30 P. A. Dub, T. Ikariya, *ACS Catal.* **2012**, *2*, 1718.
31 R. Watanabe, M. Yamauchi, M. Sadakiyo, R. Abe, T. Takeguchi, *Energy Environ. Sci.* **2015**, *8*, 1456.
32 M. Sadakiyo, S. Hata, X. Cui, M. Yamauchi, *Sci. Rep.* **2017**, *7*, 17032.
33 T. Fukushima, M. Higashi, S. Kitano, T. Sugiyama, M. Yamauchi, *Catal. Today* **2020**, *351*, 12.
34 M. Sadakiyo, S. Hata, T. Fukushima, G. Juhász, M. Yamauchi, *Phys. Chem. Chem. Phys.* **2019**, *21*, 5882.
35 M. Yamauchi, *Chem. Lett.* **2021**, *50*, 1901.
36 H. Eguchi, K. Kato, G. Juhasz, M. Yamauchi, *Catal. Sci. Technol.* **2021**, *11*, 7592.
37 M. Yamauchi, S. Hata, H. Eguchi, S. Kitano, T. Fukushima, M. Higashi, M. Sadakiyo, K. Kato, *Catal. Sci. Technol.* **2019**, *9*, 6561.
38 M. Yamauchi, H. Saito, T. Sugimoto, S. Mori, S. Saito, *Coord. Chem. Rev.* **2022**, *472*, 214773.
39 S. Kitano, M. Yamauchi, S. Hata, R. Watanabe, M. Sadakiyo, *Green Chem.* **2016**, *18*, 3700.
40 T. Fukushima, M. Yamauchi, *Chem. Commun.* **2019**, *55*, 14721.
41 T. Fukushima, M. Yamauchi, *J. Appl. Electrochem.* **2021**, *51*, 99.
42 M. Isegawa, A. Staykov, M. Yamauchi, *J. Phys. Chem. C* **2021**, *125*, 12603.
43 K. Fukutani, J. Yoshinobu, M. Yamauchi, T. Shima, S. Orimo, *Catal. Lett.* **2022**, *152*, 1583.
44 H. Eguchi, T. Kobayashi, T. Yamada, D. S. Rivera Rocabado, T. Ishimoto, M. Yamauchi, *Sci. Rep.* **2021**, in press.
45 Y. J. Wee, J. N. Kim, H. W. Ryu, *Food Technol. Biotechnol.* **2006**, *44*, 163.
46 K. Hofvendahl, B. Hahn-Hagerdal, *Enzyme Microb. Technol.* **2000**, *26*, 87.
47 M. A. Abdel-Rahman, Y. Tashiro, K. Sonomoto, *Biotechnol. Adv.* **2013**, *31*, 877.
48 L. M. Wang, B. Zhao, B. Liu, B. Yu, C. Q. Ma, F. Su, D. L. Hua, Q. G. Li, Y. H. Ma, P. Xu, *Bioresour. Technol.* **2010**, *101*, 7908.
49 M. G. Adsul, A. J. Varma, D. V. Gokhale, *Green Chem.* **2007**, *9*, 58.
50 R. P. John, K. M. Nampoothiri, A. Pandey, *Process Biochem.* **2006**, *41*, 759.
51 S. Das, J. Bhattacharyya, S. Mukhopadhyay, *Helv. Chim. Acta* **2006**, *89*, 1947.
52 P. Thakur, J. N. Mathur, R. C. Moore, G. R. Choppin, *Inorg. Chim. Acta* **2007**, *360*, 3671.
53 L. Y. Gong, Z. Y. Yang, K. Li, W. Xing, C. P. Liu, J. J. Ge, *J. Energy Chem.* **2018**, *27*, 1618.

